Korean J. Chem. Eng., 38(7), 1438-1451 (2021)
DOI: 10.1007/s11814-021-0785-5

pISSN: 0256-1115
eISSN: 1975-7220

Performance evaluation of low global warming potential working fluids as R134a alternatives for two-stage centrifugal chiller applications

Gang Li[*,**,***,†]

*Ingersoll Rand Residential Solutions, 6200 Troup Highway, Tyler, TX 75707, USA
**Ingersoll Rand Engineering and Technology Center-Asia Pacific, 200051 Shanghai, P. R. China
***School of Energy and Power Engineering, University of Shanghai for Science and Technology, 200091 Shanghai, P. R. China
(*Received 18 January 2021 • Revised 2 March 2021 • Accepted 13 March 2021*)

Abstract−With the increasing concern about climate change, the Kigali Amendment to the Montreal protocol requires parties to gradually reduce high global warming potential (GWP) hydrofluorocarbon (HFC) use by 80-85% by the late 2040s. The US Environmental Protection Agency (EPA) and EU Directive 517/2014 are also setting the ban on the use of such refrigerants. R134a, as a high GWP (GWP_{100}:1300) HFC refrigerant, is a commonly used medium pressure chiller refrigerant that will be phased out. Searching for low GWP R134a alternatives is necessary. In this study, hydrofluoroolefin blends-R513A, R513B, R515A, R515B, R516A and pure hydrofluoroolefins-R1234yf and R1234ze(E) are investigated for performance evaluation for two-stage centrifugal chiller application with a fixed cooling capacity 1,750 kW. The evaluation was conducted via a thermodynamic process model, a component sizing methodology and a life cycle environmental performance methodology. R515A, R515B and R1234ze(E) show a 25% volume capacity reduction in comparison with baseline due to their low suction density. All R134a alternatives exhibit more component heat transfer area than baseline, with 5-15% increase for the evaporator and 12-38% for the condenser. The comparison for the compressor impeller diameter shows that R513A, R513B, and R516A do not require the compressor size change from baseline, while R515A, R515B and R1234ze(E) need a more than 18% larger compressor size. R134a alternatives can provide 8.4-16.7% life cycle emission reduction in China and 14.7-27.7% in South Korea. In general, R513A, R513B and R516A are more preferable R134a drop-in options for less component modification and the same compressor can be employed directly. R516A is A2L and necessary vessel safety code protection is needed. R515A and R515B can serve as the system newly design-based interim non-flammable replacement for R134a in medium-pressure chillers with a large modification for a compressor. Gradually, with more strict regulations, R1234ze(E) can be the ultimate option in the market with less/negligible modification from R515A and R515B. For R1234yf, its poor heat transfer performance and high price can impede its application in chillers. It is anticipated that the viewpoints and insights from this study can be beneficial for the engineers, policy-makers, scholars, public and manufacturers to maintain the maximum sustainability and economic benefits.

Keywords: R513A, R513B, R515A, R515B, R516A, R1234yf, R1234ze(E)

INTRODUCTION

The past decades have witnessed an increase of global warming and serious energy challenges all over the world due to global urbanization, electrification and growing standard of living and demand for comfort [1,2]. The study from Intergovernmental Panel on Climate Change (IPCC) reveals that anthropogenic increase in greenhouse gas (GHG) concentrations and other anthropogenic forcing together have contributed more than half of the observed increase in global average surface temperature (1951 to 2010) [3]. Another study exhibits a warming trend of 0.121°±0.009 °C of the surface air temperature in China per decade from 1900 to 2015, which was enhanced during 1951-2015 as evidenced by a trend of 0.244°± 0.021 °C per decade [4]. The refrigeration sectors, from various applications, such as residential, commercial and transport, are widely recognized to substantially increase the direct GHG emissions from refrigerants and the indirect emissions associated with system lifetime energy use [5-7]. Refrigerants can be divided into four generations: the previous 1st generation Chlorofluorocarbons (CFCs), 2nd generation hydrochlorofluorocarbons (HCFCs), 3rd generation hydrofluorocarbons (HFCs) and latest generation hydrofluoroolefins (HFOs). CFCs and HCFCs, are considered for wiping out for the regulations under Montreal Protocol and the Kyoto Protocol, respectively. HFCs are the dominant generation fluids for current refrigeration systems, and R134a is the most commonly used working fluid for medium pressure system for vehicle or chiller applications. This working fluid has a good safety rating with A1, together with no flame propagation and low safety. However, it has a high global warming potential (GWP) of 1300, according to the last 5th Assessment Report published in 2013 [8]. Recent regulations put strict timeframes towards the protection and preservation of the environment. In Oct. 2016, the main member countries of the Montreal Protocol had one meeting for amendment, with the focus to phasing down HFCs and HCFCs with the target of reducing net earth warming by 0.5 °C by the year 2100 to protect the ozone layer [9]. The amendment adds powerful GHG HFCs

†To whom correspondence should be addressed.
E-mail: gangli166@gmail.com
Copyright by The Korean Institute of Chemical Engineers.

to the list of substances controlled under the Protocol and which are to be phased down. Under the amendment, Montreal Protocol parties are required to gradually reduce HFC (such as R134a) use by 80-85% by the late 2040s. First reductions by most developed countries were expected in 2019. Most developing countries will follow suit by a freeze of HFCs consumption levels in 2024, and in 2028 for some of them. In addition, the United States (US)'s Environmental Protection Agency (EPA) has decided to systematically phase out HFCs to 50% by 2024, 80% by 2029, and 100% by 2034 [10]. What's more, the EU Directive 517/2014 [11,12] has a ban on the use of high-GWP refrigerants for various applications. A GWP_{100} (up to 150) is generally considered as a reference in domestic stand-alone systems and freezers for commercial use and in vehicle air-conditioning appliances. With the growing concern about current HFC refrigerant-R134a from various regulations, a search for more environmentally-friendly fluids (including aforementioned latest generation HFOs) has begun.

Potential alternatives to R134a should have significantly lower GWP, and they should operate at similar system pressures, show good heat transfer, equivalent or better system performance and good chemical stability. A close scrutiny of the development of alternative refrigerants shows the most R134a alternatives are pure HFCs or HFOs, hydrocarbons (HCs), inorganic refrigerants (R7XX series) and blends based on the aforementioned fluids. It should be mentioned that HFO compounds have become an alternative to HFC refrigerants in the era of the fight against global warming. An extensive investigation of R134a alternatives under various applications, such as vehicle applications, domestic refrigerators, heat pumps and chillers, has been performed in recent years. For automobile air conditioning application, a series of studies have been conducted. Navarro et al. [13] conducted the tests for R134a, R290, and R1234yf under different operation conditions. They reported that R290 can achieve improvement for both compressor and volumetric efficiency in comparison with R134a. Zhao [14] performed an experimental comparison between R1234yf and R744. R744 can demonstrate better operability under low-temperature conditions. Jignesh [15] conducted a theoretical study of fluids R152a, R290, R407C, R600a, R410A, R404A, and R1234yf for performance comparison with R134a. R1234yf exhibits the most suitable R134a alternative from the viewpoint of thermodynamic aspects. Aized and Hamza [16] thermodynamically investigated R134a, R152a, and R1234yf under an evaporating temperature of 5 °C and condensing temperature of 50 °C, respectively. Results showed that R152a exhibits approximately 7.7% power reduction from R134a. R152a achieves a 5.33%, 5.16% and 4.92% higher coefficient of performance (COP) from R134a under the engine speeds of 1,000, 2,000 and 3,000 rpms, respectively. R134a alternatives for domestic refrigerators and related applications have also been investigated in recent years. Li et al. [17] compared R717, R600a, and R1234yf with R134a in domestic refrigerators, and results showed that R1234yf has similar drop-in performance to R134a. Aprea et al. [18] reported the results of a comparative experimental analysis between R134a and R1234ze(E) in a household refrigerator and revealed that, in particular, the cycle working with R1234ze(E) with the optimal charge shows an energy saving of 9%. Aprea et al. [19,20] also investigated the test for binary mixture, such as R1234yf/R134a (90/10 wt%), R1234ze(E)/R134a mixture (90/10 wt%) in a domestic refrigerator. R1234yf/R134a mixture leads a 17% reduction for the life cycle climate performance index from R134a, and R1234ze(E)/R134a mixture could achieve energy saving of 14.1% on R134a and of 8.92% on pure R1234ze(E). Mota Babiloni et al. [21] conducted a drop-in test for R450A, an R1234ze(E)/R134a mixture for the vapor compression system with a variable compressor component. With proper setting for evaporating temperature and condensing temperature, R450A can lead to a 6% drop in the cooling capacity an increase of average 1% for system coefficient of performance from the baseline R134a. An overview of low GWP mixtures for the replacement of HFC refrigerants R134a can also be found in Reference [22]. In addition, there are also some studies for R1234ze(E) and R515B for heat pump systems with heating production temperatures up to 90 °C and R515B becomes a promising non-flammable alternative (A1) for heat pumps [23]. Regarding the chiller applications, Johnson and Kasai [24] conducted drop-in tests for a 200 Ton R134a air-cooled screw chiller with R1234ze(E). Their report showed that R1234ze(E) has a 6% higher COP than R134a under 35 °C ambient conditions. R1234ze(E) can lead to a 23% lower cooling capacity, and a larger displacement compressor is suggested to replace to match the capacity of R134a. Ueda et al. [25] performed another drop-in test using R1234ze(E) in an R134a centrifugal chiller. Compatibility of products related to lubrication and the performance of the chiller via full- and partial-load had been analyzed. The test report under full load condition indicated that cooling capacity and COP are reduced by approximately 29% and 3%, respectively, at the same inlet volumetric flow rate. Brasz [26] made the capacity and performance prediction of a centrifugal compressor using an ideal cycle and a thermodynamic property calculation for R1234ze(E). It was found that R1234ze(E) can lift the efficiency of the chiller due to the low rotational speed and viscous loss compared to conventional centrifugal compressors, which are larger than the centrifugal compressor used in the conventional chiller. However, it was also suggested that a condenser redesign is necessary to prevent a pressure drop from the condenser. Mota-Babiloni et al. [27] conducted drop-in tests of R1234yf and R1234ze(E) to replace R134a in a vapor compression plant. Results showed that the volume efficiency, cooling capacity, and COP could be decreased compared with those of R134a, and the use of an internal heat exchanger could help to reduce the COP difference. Sethi et al. [28] analyzed the theoretical evaluations of low GWP refrigerants R1234yf, R1234ze(E) and R515A in medium pressure centrifugal chiller applications to replace R134a. Results show that they match the efficiency of R134a while providing significant reduction in direct emissions. Though extensive studies have been performed for various applications, there is a lack of heat exchanger sizing and heat transfer performance evaluation for different fluids, especially for chiller studies.

With the development of new low GWP working fluids from chemical manufacturers as R134a alternatives for chiller applications for the past several years to relieve the issues of global warming, a comprehensive performance evaluation for chiller system is required. The new coming R134a alternatives, mostly the HFO blends, such as products of R513B, R515B, and R516A, have not been carefully and systematically investigated for chiller applications

based on the literature review. In addition, the aforementioned existing studies are lacking the investigation from heat transfer performance and system component sizing comparison for different fluids. Thus, for current study, a comprehensive R134a alternative chiller investigation for both the system level performance and component performance covering with heat exchanger and compressor sizing, heat transfer characteristics will be conducted. More importantly, the life cycle environmental performance will also be evaluated. The R134a alternatives will be extended from R515A, R1234yf, R1234ze(E) to other new fluids such as R513A, R513B, R515B and R516A. Azeotropic mixture was considered and zeotropic was not considered since the possible leakage in chiller system will degrade the system performance. It is anticipated that the viewpoints from this study can be beneficial for the engineers, policy-makers, and manufacturers to maintain the maximum system thermal performance delivery with consideration of environmental protection and economic benefits as well.

This paper is organized as follows: Section 2 introduces the working fluid selection and comparison. Section 3 shows the two-stage centrifugal chiller system description, and Section 4 introduces the two-stage centrifugal chiller thermodynamic model, component size methodology, and environmental performance evaluation methodology. Section 5 discusses the results for system and component performance. Section 6 summarizes the perspectives, directions and conclusions towards the sustainable target.

PROPERTIES OF REFRIGERANTS SELECTED

In Table 1 is reported a comparison of the main characteristics between baseline R134a and other refrigerants with low GWP [29] for assessment the suitability of its alternatives. R513A and R513B can lead to ~55% GWP reduction, and R515A and R515B more than 70%, R516A 92% and two HFOs more than 99%.

In Table 1 is shown a comparison of the normal boiling point (NBP), and refrigerants of R513A, R513B, R516A and R1234yf have a close value to baseline R134a. R134a exhibits a higher critical pressure than its alternatives. R516A, R1234yf, R1234ze(E) have the risk of flammability (A2L), which means strict refrigerant charge limit and protection approaches are needed for the guarantee of safety. R1234yf displays the lowest liquid thermal conductivity while R134a highest. In Fig. 1 is shown the T-s and P-($-T_{sat}^{-1}$) diagrams for various refrigerants. The width of the T-s dome indicates the latent heat of vaporization, and R1234yf is the narrowest while the R134a the widest. R513A, R513B, R516A and R1234yf display a closer vapor pressure curve to R134a over a wide range of temperature than refrigerants of R515A, R515B and R1234ze(E), especially under the operating condition map (evaporating temperature: 6 °C, condensing temperature: 36 °C).

TWO-STAGE CENTRIFUGAL CHILLER SYSTEM DESCRIPTION

As shown in Fig. 2, an economizer is included in a two-stage centrifugal chiller configuration. The benefits of the economizer are as follows: (1) The inlet temperature of the 2nd stage compressor can be reduced; thus polytropic head/enthalpy rise required for the 2nd stage compressor can be decreased, (2) the quality of working fluids at the inlet of evaporator can be decreased via reverting flash gas into the 2nd compressor; thus the chiller efficiency can be increased, (3) the 2nd compressor inlet gas density increases; thus

Table 1. Main characteristics of R134a and its alternatives

	R134a	R513A	R513B	R515A	R515B	R516A	R1234yf	R1234ze(E)
Composition (Mass %)	Pure	R1234yf/ R134a (56.0/44.0)	R1234yf/ R134a (58.5/41.5)	R1234ze(E)/ R227ea (88.0/12.0)	R1234ze(E)/ R227ea (91.1/8.9)	R1234yf/ R134a/R152a (77.5/8.5/14.0)	Pure	Pure
Molecular mass (g/mol)	102.0	108.4	108.7	118.73	117.5	102.6	114.04	114
ASHARE Std 34 safety class	A1	A1	A1	A1	A1	A2L	A2L	A2L
ODP	0	0	0	0	0	0	0	0
AR5 $GWP_{100\text{-}year}$	1300	573	540	403	299	131	1	1
Critical temperature (°C)	101.1	96.5	95.5	108.7	108.88	96.8	94.7	109.4
Critical pressure (kPa)	4,059	3,766	3,660	3,565	3,584	3,615	3,382	3,636
NBP (°C)	−26.1	−29.2	−29.2	−18.7	−18.8	−29.4	−29.45	−18.95
Liquid density[a] (kg/m^3)	1,206.7	1,134.2	1,131	1,187.2	1,180.9	1,069.2	1,091.9	1,163.1
Vapor density[a] (kg/m^3)	32.4	37.628	37.32	27.176	26.948	34.5	37.9	26.3
Liquid c_P[a] (kJ/kgK)	1.4246	1.4117	1.417	1.3610	1.3673	1.4563	1.3921	1.3856
Vapor c_P[a] (kJ/kgK)	1.0316	1.0565	1.059	0.966	0.96859	1.0890	1.0533	0.9758
Liquid therm. cond.[a] (mW/m·K)	81.134	69.931	69.512	72.895	73.244	70.092	63.538	74.216
Vapor therm. cond.[a] (mW/m·K)	13.825	14.032	14.037	13.928	13.933	14.380	13.862	13.590
Liquid viscosity[a] (μPa s)	194.89	166.00	165.03	194.12	193.13	154.84	152.91	190.5
Vapor viscosity[a] (μPa s)	11.693	11.626	11.618	12.169	12.185	11.416	11.425	12.228
Latent heat[a] (kJ/kg)	177.79	156.35	155.6	160.3	162.01	164.01	145.4	166.92
Latent heat at boiling point (kJ/kg)	216.98	194.48	193.55	187.96	189.95	202.77	180.22	195.61

[a]Under 25 °C conditions. All properties were obtained using REFPROP

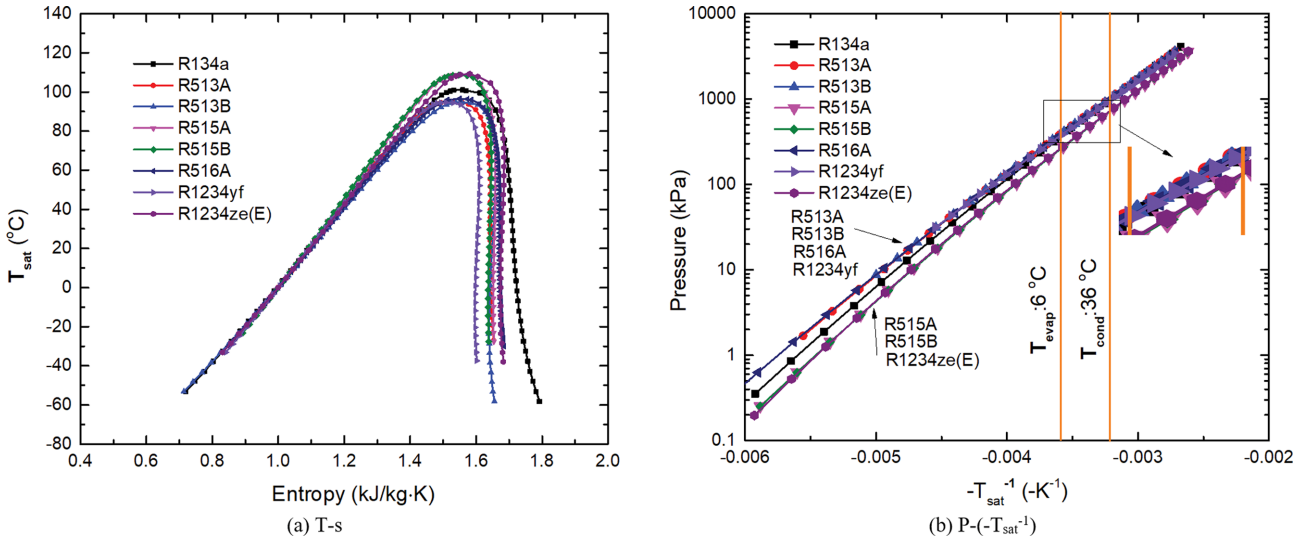

(a) T-s (b) P-($-T_{sat}^{-1}$)

Fig. 1. T-s and P-($-T_{sat}^{-1}$) diagram.

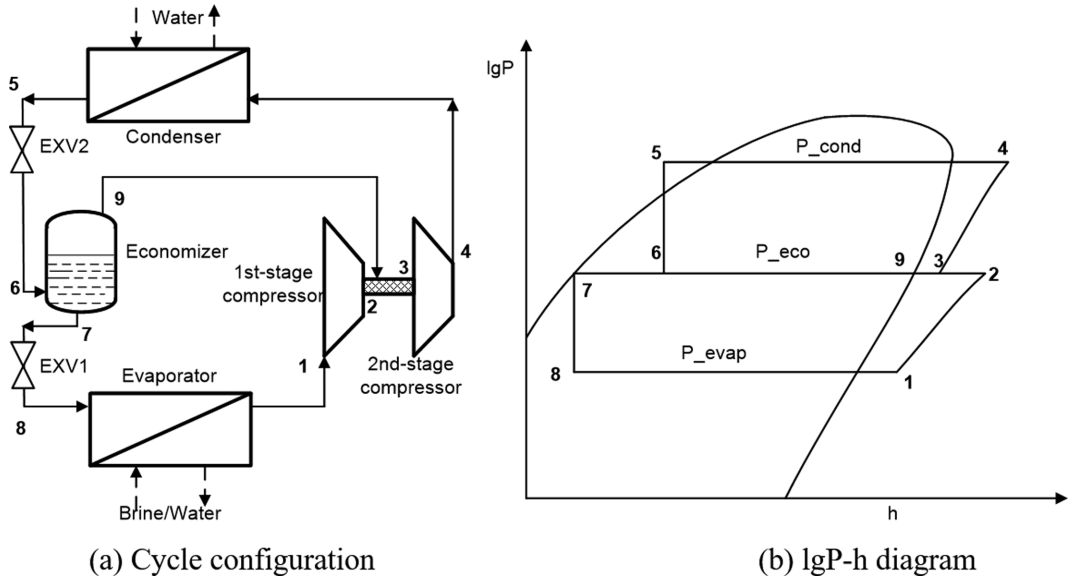

(a) Cycle configuration (b) lgP-h diagram

Fig. 2. Schematics of two-stage centrifugal chiller system.

the 2nd compressor size can be decreased. The process working fluid is initially under evaporating pressure at point 1 and is fed to 1st stage compressor and compressed at point 2. Then the fluid with superheated vapor state at point 2 and another fluid stream with saturated vapor state at point 9 from the outlet of economizer mix and become mixed fluid point 3. Fluid at point 3 is fed to the 2nd compressor and compressed to point 4. Then it is sent to a condenser to remove the heat of compression and becomes subcooled point 5. After expansion with a sudden reduction in pressure, the refrigerant changes into a vapor/liquid mixture at point 6. The stream fluid at point 6 is then flowed into the economizer. Then it is divided into two sub-flows, with one flow at saturated vapor state point 9 towards the compressor side and another saturated liquid state point 7. After another expansion for fluid at point 7, it becomes the low quality at point 8. Then the fluid with low pressure state is passed into the evaporator and generates a refrigeration effect. For this cycle, there are two shell-and-tube heat exchangers (condenser and evaporator) and one fluid tank (economizer). For the current study, an evaluation of the thermal performance has been focused only on the condenser and on the evaporator). All heat exchangers are counter-current shell and tube heat exchangers with the working fluid at the shell side.

MODELS AND METHODOLOGY

In this section, different models/methodologies for chiller thermodynamic process, component sizing and life time environmental performance, are presented. In addition, the performance evaluation

methodology is also revealed.

1. Chiller Thermodynamic Process and System Performance Evaluation

Before the simulation, the evaporating temperature and condensing temperature are pre-set. Thus, pressure for evaporating and condensing can be determined from software REFPROP [29]. The pressure for the economizer can be determined via:

$$P_{eco}=\sqrt{P_{evap}\cdot P_{cond}} \tag{1}$$

P_{evap} is the pressure for the evaporator and P_{cond} is the pressure for the condenser side. Thus, as shown in Fig. 2, the saturated vapor point 9 and saturated liquid point 7 corresponding to P_{eco} can be obtained. Point 8 with pre-set pressure P_{evap} and the same enthalpy to point 7 can also be determined for thermal properties. In addition, with the pre-set superheat degree, the point 1 thermal properties can be determined. With the fixed cooling capacity, the evaporator side refrigerant mass flow rate can be calculated as:

$$\dot{m}_1=Q_{evap}/(h_1-h_8) \tag{2}$$

The 1st stage compressor power, which can compress the vapor state refrigerant from point 1 to high pressure state point 2, is calculated as:

$$W_{comp1}=\dot{m}_1(h_2-h_1)=\dot{m}_1(h_{2s}-h_1)/\eta_{comp1} \tag{3}$$

η_{comp1} is the isentropic efficiency for the 1st stage compressor and $\dot{m}_1$ is the mass flow rate for the 1st stage compressor.

Based on the condensing pressure and pre-set subcooling, point 5 can be determined for its thermal properties. With the pressure of P_{eco} and same enthalpy to point 5, thermal properties for point 6 can also be obtained.

If $\dot{m}_2$ is the mass flow rate for the 2nd compressor, based on the energy balance for the economizer, $\dot{m}_2$ can be calculated from the below equation,

$$\dot{m}_2h_6=\dot{m}_1h_7+(\dot{m}_2-\dot{m}_1)h_9 \tag{4}$$

Point 3 with the pressure of P_{eco} as the 2nd compressor inlet, can be obtained as,

$$\dot{m}_2h_3=\dot{m}_1h_2+(\dot{m}_2-\dot{m}_1)h_9 \tag{5}$$

The 2nd stage compressor power, which can compress the vapor state refrigerant from point 3 to high pressure state point 4, is calculated as:

$$W_{comp2}=\dot{m}_2(h_4-h_3)=\dot{m}_2(h_{4s}-h_3)/\eta_{comp2} \tag{6}$$

The condenser side heating capacity is given by:

$$Q_{cond}=\dot{m}_2(h_4-h_5)=\dot{m}_{cooled}(h_{cooled,\,out}-h_{cooled,\,in}) \tag{7}$$

$\dot{m}_{cooled}$ is the condenser side cooled water mass flow rate.

The evaporator side cooling capacity is given by:

$$Q_{evap}=\dot{m}_1(h_1-h_8)=\dot{m}_{chill}(h_{chill,\,in}-h_{chill,\,out}) \tag{8}$$

$\dot{m}_{chill}$ is the evaporator side chilled water mass flow rate for loadings.

The total compressor work needed is given by:

$$W_{comp}=W_{comp1}+W_{comp2} \tag{9}$$

System coefficient of performance is calculated as:

$$COP=\dot{Q}_{evap}/W_{comp} \tag{10}$$

For this section, to simplify the calculation, the pressure drop throughout the heat exchangers is neglected. The rating evaporating temperature is pre-set as 6 °C and condensing 36 °C, respectively. 1,760 kW is fixed as the cooling capacity. 1st stage compressor superheating is set to be 5 K and condensing subcooling degree is set 3 K, respectively. The compressor isentropic efficiency for both compressors is set to be 80%. For the thermodynamic process, all the potential energy, kinetic energy, and pressure drops across the heat exchangers for the system are neglected. The expansion in the throttling valve is the isenthalpic process.

2. Component Sizing

For the current study, the heat exchangers (mainly for evaporator and condenser, and the economizer is not considered here) are pre-set as the counter-current flow shell and tube type, with one-pass in shell and two-pass in tubes. The heat source/heat sink fluid (i.e., chilled water/cooled water) is in the tube side and the working fluid is in the shell side. The heat exchanger must satisfy the process requirements with allowable pressure drops (<30 kPa in the current study). The working fluid heat transfer coefficient and heat exchanger area will be compared. For the compressors, the specific diameter, pressure ratio, head, and tip speed will be compared for different fluids. The cooling capacity is pre-set to be 1,750 kW and the heat exchangers are performed for design based on the rating condition.

2-1. Heat Exchangers

In both the evaporator and condenser the secondary fluid is single phase liquid water. In the evaporator, the refrigerant fluid at the shell side enters as saturated vapor and leaves as super-heated; in the condenser the refrigerant fluid enters as super-heated vapor and leaves as subcooling liquid. First, the tube length L_{tube} and the shell diameter D_s can be pre-set initially based on the engineering experience based on the type of working fluid.

With the tube geometry determined, the total number of tubes can be predicted in fair approximation as function of D_s by taking the shell circle and dividing it by the projected area of the tube layout pertaining to a single tube A_1,

$$N_T=(CTP)\pi D_s^2/(4A_1) \tag{11}$$

CTP is the tube count calculation constant that accounts for the incomplete coverage of the shell diameter by the tubes [27]. Its value is 0.93 for one-tube pass, 0.90 for two-tube pass and 0.85 for three-tube pass, correspondingly. Here, two-tube pass is selected.

$$A_1=(CL)P_T^2 \tag{12}$$

P_T is the tube pitch and CL is the tube layout constant, with the value to be 1 for 90° and 45°, and 0.87 for 30° and 60°, correspondingly [30]. Here 30° is set. Here tube pitch is set as 22 mm. Tube external diameter d_{out} is set as 19 mm (0.019 m).

The heat transfer area is obtained by,

$$A_{HX}=N_TL_{tube}(\pi d_{out})N_s \tag{13}$$

L_{tube} is the tube length, d_{out} is the tube external diameter, and N_s is the number of shells per heat exchanger. Here N_s is 1.

For practical design applications, most heat exchangers are using

Table 2. Part-load conditions for rating for Integrated Part-Load Value (IPLV) [32]

Evaporator (All types)	
100% Load LWT [°C]	7
0% Load LWT [°C]	7
Flow rate [m^3/(h·kW)]	0.172
F.F.A. [m^2·°C/kW]	0.018
Water-cooled condenser	
100% Load EWT [°C]	30
75% Load EWT [°C]	26
50% Load EWT [°C]	23
25% Load EWT [°C]	19
Flow rate [m^3/(h·kW)]	0.215
F.F.A. [m^2·°C/kW]	0.044

LWT - Leaving water (liquid) temperature
EWT - Entering water (liquid) temperature
F.F.A - Fouling Factor Allowance

commercially available tools or service. The software is developed by Heat Transfer and Fluid Flow Service (HTFS) and Heat Transfer Research Inc. (HTRI). Such programs incorporate multiple design codes and standards from the American Society of Mechanical Engineers (ASME), Tubular Exchangers Manufacturers Association (TEMA) and the International Standards Organization (ISO). HTRI software [31] is utilized for heat transfer calculation. TEMA type BEU with horizontal orientation is chosen and tube is the plain type with layout angle 30° and wall thickness is 2.2 mm. The tube material is 304 stainless steel (18 Cr, 8Ni). The thermal fluid process condition inputs are determined from aforementioned section (*Chiller Thermodynamic Process and System Performance Evaluation*) for water side/refrigerant side pressure/temperature/vapor quality/mass flow rate conditions. The heat exchanger thermal calculation in HTRI is based on the rating condition (100% load) from Table 2 [32] based on China chiller standard. The fluid information can be obtained from the HTRI fluid package REFPROP.

In HTRI, baffles play a significant role in shell and tube heat exchanger assembly. They can help to support for the tubes, enable a desirable velocity to be maintained for the shell-side fluid flow, and prevent the tubes from vibrating. More importantly, they can push the shell-side flow to move forward across the tube bundle, providing the fluid disturbance with zigzag pattern between the tube bundles, which enhances the turbulence intensity, the local mixing, and heat transfer coefficient. Here the single segmental baffles are selected. The baffle cut ratio is 25% of the shell ID with cut orientation as perpendicular. A reasonable setting for baffle spacing is needed. With all needed information input into the system and run, the shell-side, tube-side and overall heat transfer heat transfer coefficient can be obtained. Therefore, with U_f obtained, the required heat exchanger heat transfer area based on fluid heat transfer characteristics can be obtained via,

$$A_{HX,\,req} = Q/(U_f \cdot LMTD \cdot F_T) \tag{14}$$

$A_{HX,req}$ is the heat transfer area, Q is the heat flow, F_T is the temperature factor correction from the software, and LMTD is the log-mean temperature difference. Proper setting for shell diameter and tube length should be selected to make sure δ in the range of 0 to 10%. For the fair comparison, all working fluids should have the same value of δ.

$$\delta = (A_{HX} - A_{HX,\,req})/A_{HX,\,req} \tag{15}$$

During the HTRI simulation, proper arrangements for baffle inlet spacing, nozzle location, and nozzle geometry for shell and tube side should be performed carefully. With the satisfied value for δ within the needed range, the shell side working fluid heat transfer performance, overall heat transfer performance and heat exchanger area can be obtained for comparison.

2-2. Compressors

For the current cycle configuration, there are two compressors. The concept of the specific speed comes from similarity considerations and has been proposed [33]. In this study, it is anticipated that the volume flow rate, compressor rational speed and head (or the isentropic enthalpy life) can be combined in a non-dimensional group. It has been revealed that dimension of m^3/s can be obtained from the volumetric flow rate (V_{ref}). The dimension of s^{-1} can be obtained for the rotational speed (N), considering taking the ratio of the head (H) to the power ¾ and the flow to the power ½:

$$H^{3/4}/V_{ref}^{1/2} = (m^2/s^2)^{3/4}/(m^3/s)^{1/2} = s^{-1} = N \tag{16}$$

Then the non-dimensional specific speed n_s can be defined as

$$n_s = N \cdot V_{ref}^{0.5}/H^{0.75} \tag{17}$$

Thus, the non-dimensional specific diameter d_s can be expressed as:

$$d_s = D \cdot H^{0.25}/V_{ref}^{0.5} \tag{18}$$

Then combining such equations we can simply get the following equations:

$$N = 0.76 \cdot H^{0.75}/V_{ref}^{0.5} \tag{19}$$

$$D = 3.4 \cdot V_{ref}^{0.5}/H^{0.25} \tag{20}$$

For the expressions, a specific speed on 0.76 and a specific diameter of 3.4 are used to present the compressor speed N and diameter D for 1st and 2nd compressors.

The compressor ratio for each compressor can be calculated as:

$$PR = P_{dis}/P_{suc} \tag{21}$$

P_{dis} is the discharge pressure and P_{suc} is the suction pressure for the corresponding compressors. The working fluid properties are used from the software HTRI REFPROP package. The 1,750 kW cooling capacity is fixed for all working fluids.

3. Life Cycle Environmental Performance Evaluation

Prior to the whole environmental performance, the refrigerant charge should be investigated. Based on the literature, there are already extensive studies for refrigerant distribution for the vapor compression cycle systems, and the evaporator and condenser together contribute the largest sector (~70% by mass). Others go for the liquid lines/pipes, compressors, etc. From the study from [34], for R134a, the charge amount is 0.355 kg for per nominal ton cooling capacity. The current 1,750 kW cooling capacity for R134a can be

calculated for 177.4 kg refrigerant charge. For the rating condition, preliminary results show that two-phase region domains ~97% capacity for the evaporator and ~90% for the condenser for most fluids. Thus, only two phase region is studied here. The two phase region refrigerant charge is calculated as,

$$M_{tp}=\pi\cdot(D_{tp}/2)^2\cdot\int_0^{l_{tp}}[\varepsilon\rho_g+(1-\varepsilon)\rho_l]dl \quad (22)$$

The calculation of two-phase length can be determined from HTRI with two-phase inlet/outlet setting. D_{tp} is the characteristic diameter for the shell, and it is same to shell diameter D_s. ρ_g is the density of gas and ρ_l the liquid. ε is the void fraction, which is the ratio of cross-sectional area occupied by gas section to that of the liquid section, and it can be calculated based on Tandon calculating model [35] as follows,

$$50<Re_L<1125,\ \varepsilon=[1-1.928Re_L^{-0.315}/F(X_{tt})+0.9293Re_L^{-0.315}/F(X_{tt})^2] \quad (23)$$

$$Re_L\geq1125,\ \varepsilon=[1-0.38Re_L^{-0.088}/F(X_{tt})+0.361Re_L^{-0.176}/F(X_{tt})^2] \quad (24)$$

$$F(X_{tt})=0.15[1/X_{tt}+2.85/(X_{tt})^{0.476}] \quad (25)$$

$$X_{tt}=(1-x)/x\cdot[(\mu_l/\mu_g)^{0.2}\cdot(\rho_g/\rho_l)]^{0.5} \quad (26)$$

To simplify the process, all other fluid charge can be obtained via:

$$M_{Alter}=M_{R134a}\cdot(\Sigma M_{tp,\,Alter}/\Sigma M_{tp,\,R134a}) \quad (27)$$

ΣM_{tp} is the total two phase charge amount including both the condenser and evaporator.

Based on the China chiller standard [32], the chiller seasonal performance index-integrated part-load value (IPLV) is given by,

$$IPLV=0.023\ A+0.415\ B+0.461\ C+0.101\ D \quad (28)$$

where, A=COP at 100% load (kW/kW); B=COP at 75% load (kW/kW); C=COP at 50% load (kW/kW) and D=COP at 25% load (kW/kW). Note that 0.023, 0.415, 0.461 and 0.101 represent the weighting factor for the index (loading×hour) under 100%, 75%, 50% and 25% loading condition, respectively. For China, taking the typical chiller annual operating hours (1,366 h) [36], for example, and if t_1, t_2, t_3 and t_4 can represent the loading time under the four conditions, they can be obtained as:

$$t_1+t_2+t_3+t_4=1366 \quad (29)$$

$$t_1/(t_1+0.75t_2+0.5t_3+0.25t_4)=0.023 \quad (30)$$

$$0.75t_2/(t_1+0.75t_2+0.5t_3+0.25t_4)=0.415 \quad (31)$$

$$0.5t_3/(t_1+0.75t_2+0.5t_3+0.25t_4)=0.461 \quad (32)$$

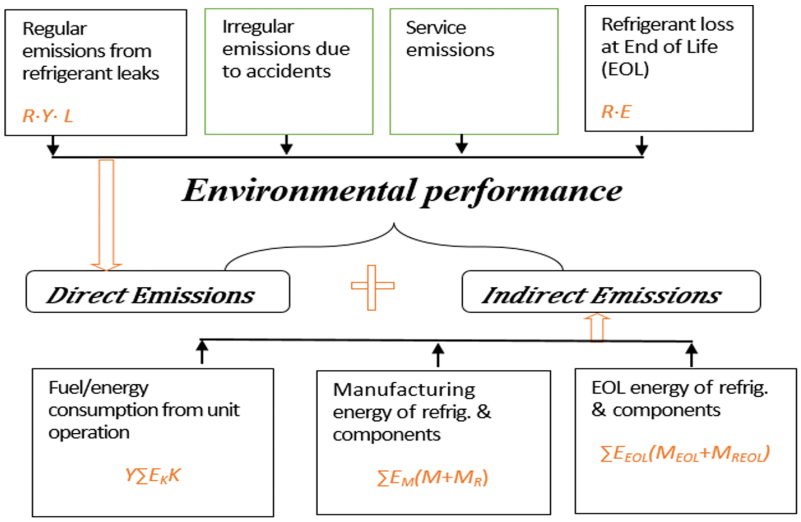

EI=Direction Emissions+ Indirect Emissions
Direction Emissions= $R\cdot(YL+O_{SA}+E)$
Indirect Emissions= $Y\sum E_K K+\sum E_M(M+M_R)+\sum E_{EOL}(M_{EOL}+M_{REOL})+\sum E_{Other}$
R – Working fluid emission factor, such as GWP, etc., kg/kg;
Y – Lifetime, in years
L – Annual regular emissions due to refrigerant leaks from the system during operation, kg/year;
O_{SA}– Other regular emissions due to leakage in assembly plants, irregular emissions due to accidents and service emissions from servicing operations during system whole life cycle, kg;
E – Refrigerant loss at the End-of-Life (EOL) of the unit, kg;
K – Annual chiller operating season energy consumption from the unit operation, kWh/year;
M_R, M– Mass of refrigerants and components for manufacturing purpose, kg;
M_{REOL}, M_{EOL}– Mass of refrigerants and components for EOL energy purpose, kg;
E_K – Equivalent emission index for energy consumption from unit operation, kg/kWh;
E_M – Equivalent emission index material of refrigerants or components for manufacturing energy purpose, kg/kg;
E_{EOL} – Equivalent emission index material of refrigerants or components for EOL energy purpose, kg/kg;

Fig. 3. Chiller system environmental impact evaluation methodology.

Thus, the annual chiller electricity energy consumption can be listed as,

$$K=Q_{evap}(t_1/A+0.75t_2/B+0.5t_3/C+0.25t_4/D) \quad (33)$$

From the aforementioned equations, the fluid refrigerant charge amount and annual energy consumption can be obtained. The following will introduce the chiller environmental performance evaluation methodology, as is shown in Fig. 3. The whole emissions include the direct and indirect emissions. As to the direct emissions, annual refrigerant loss from gradual leaks during usage (R·Y·L), refrigerant loss at end of life (EOL) disposal of the unit (R·E), irregular emissions from accidents and service emissions ($R\cdot O_{SA}$) are the main contributors. For the current chiller, the commonly used refrigerant R134a (GWP_{100}=1300) and its low GWP alternatives are adopted. Regarding the indirect emissions, it includes the emission due to fuel/energy consumption (i.e., electricity) for system operation, emission due to manufacturing and EOL life energy of refrigerant and components (component materials and weight information can be obtained from HTRI software), and other emissions such as energy consumption for raw material transport for system construction and energy consumption for disposal and recycled solid waste for decommission. Once all databases are provided, it can conduct the calculations for all kinds of energy consumption aspects. Then other indirect and direct emissions can also be combined for final delivery. The regular annual leakage rate is set to be 10% and the system whole lifetime is 15 years. The working fluid loss EOL is set to be 15%.

RESULTS AND DISCUSSION

1. Chiller System Thermal Performance for Different Working Fluids

Different working fluids, R134a and its alternatives, such as HFO blends (R513A, R513B, R515A, R515B, R156A) and pure HFOs (R1234yf and R1234ze(E)) were investigated. As shown in Fig. 4, the COP for the two-stage chiller systems is fairly close (within 1%) for all alternatives from the baseline R134a. For the unit capacity by mass, the R134a is 178.97 kJ/kg, and all alternatives exhibit ~10% or lower, with R1234yf lowest (20% lower). For the volume capacity, R513A, R513B and R516A can achieve a 4%, 4% and 1% higher than baseline (baseline volume capacity: 3,088 kJ/m^3) since they all have a higher suction density (20.45, 20.53, and 18.93 kg/m^3) than baseline R134a (17.26 kg/m^3). R515A, R515B and R1234ze(E) show a 25% capacity reduction in comparison with baseline due to their low suction density (~14.3 kg/m^3). From this comparison it is found that if drop-in tests are performed for such three fluids, 25% cooling capacity may be lost. It is recommended that a larger compressor is needed for R515A, R515B and R1234ze(E) to obtain a similar cooling capacity to the baseline. In addition, the condensing pressure for such three fluids is similar, and all are lower than the baseline.

Regarding the working flow rate, R134a has a 9.83 kg/s for 1st stage compressor mass flow rate, and due to the flash gas from the economizer adding to the 2nd stage system, an 11.2% higher mass flow rate (10.93 kg/s) is achieved for the 2nd stage system. The calculation also shows that the 1st stage compressor volume flow rate of R134a is 0.5697 m^3/s, while the 2nd is only 0.4104 m^3/s, which is

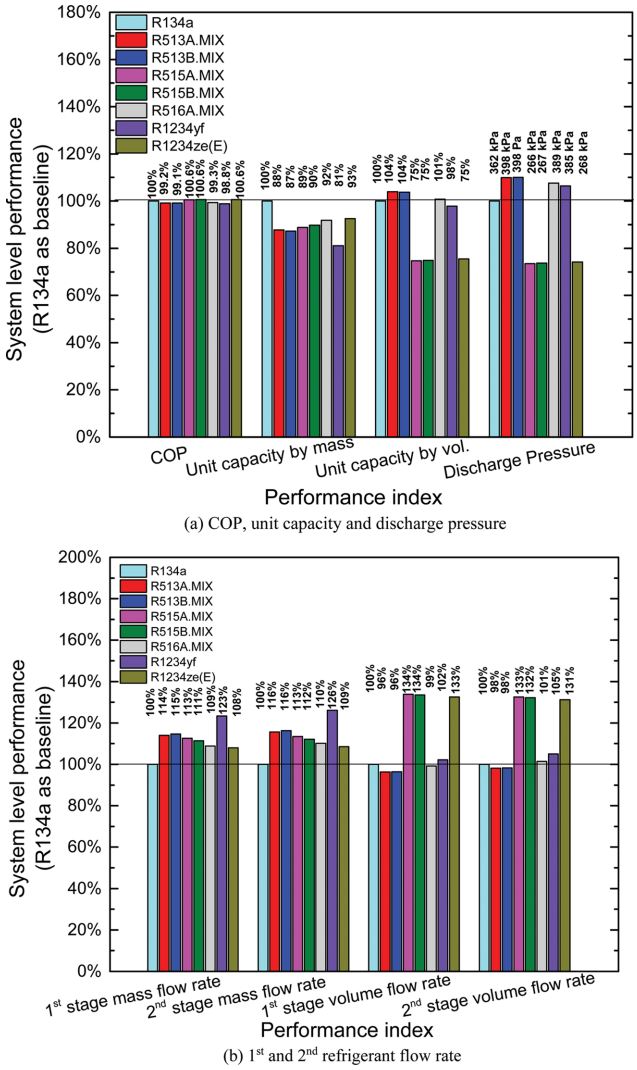

(a) COP, unit capacity and discharge pressure

(b) 1st and 2nd refrigerant flow rate

Fig. 4. System level chiller performance.

lower than the 1st stage. As mentioned in section 3, the 2nd compressor inlet gas density increases, which is 26.65 kg/m^3, much higher than the 1st stage 17.26 kg/m^3; thus the volume flow rate can be decreased. Regarding the R134a alternatives, as shown in Fig. 4, in general, with the fixed cooling capacity, all alternatives have a ~10% or higher mass flow rate, and the 1st stage and 2nd stage have a similar trend. R1234yf has a 23% higher mass flow rate than R134a. This can be explained from Fig. 1. The width of the T-s dome is representing the latent heat of vaporization, and a widened curve usually means a larger value of vaporization heat. R1234yf is the narrowest and R134a is the widest; therefore, with a fixed cooling capacity, R134a displays the lowest mass flow rate.

In addition, as for the volume flow rate, among the R134a alternatives, R515A, R515B and R1234ze(E) display a ~30% higher value due to their lower suction density and other fluids are close to the baseline.

2. Chiller Heat Transfer Performance and Component Sizing Comparison for Different Working Fluids

In this section, the two-stage centrifugal chiller heat transfer per-

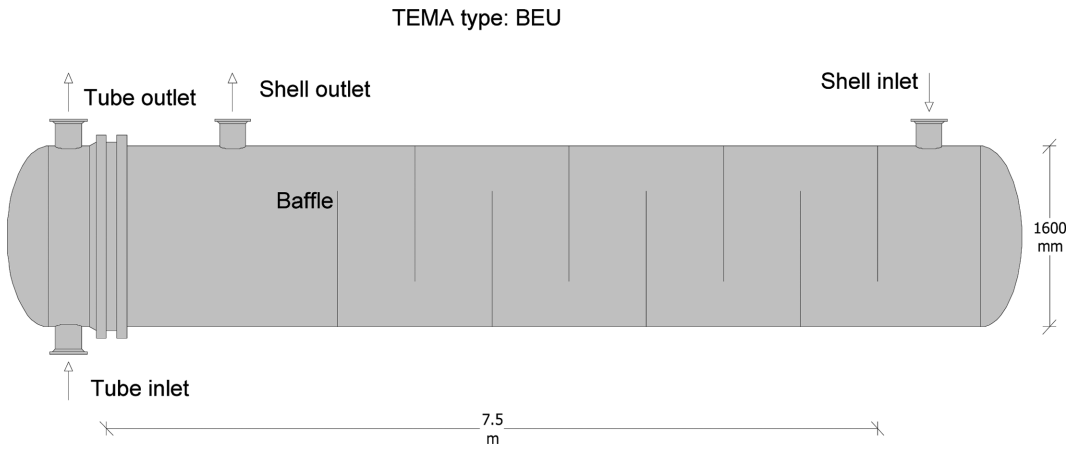

Fig. 5. Shell and tube type.

formance and component sizing comparison for different working fluids will be discussed. The heat transfer performance is mainly discussed for evaporator and condenser shell side with R134a and its alternatives. The tube side is water with sensible state and its heat transfer performance does not vary much for the heat exchanging processes. The component sizing is mainly for evaporators/condenser with heat exchanger area and compressor with impeller size comparison for different working fluids. As shown in Fig. 5, the heat exchangers are designed as TEMA E type shell-and-tube heat exchangers with one shell pass and one tube pass. A 30° triangular tube layout is used, a U-tube. The advantage of a U-tube heat exchanger is that because one end is free, the bundle can expand or contract in response to stress differentials. In addition, the outsides of the tubes can be cleaned, as the tube bundle can be removed. Once again it is mentioned that in order to avoid leakage of working fluid in such heat exchangers, zeotropic mixtures are not considered since they can result in undesirable composition shifts, thus bringing serious system performance degrading.

2-1. Evaporator and Condenser

During the heat transfer and component sizing process in HTRI, proper pre-set for evaporator and condenser is needed. In general, ~7.5 m (or longer in a reasonable range) tube length with 1,600 mm (or higher in a reasonable range) shell internal diameter is needed for evaporator. Baffle spacing is around 750 mm for evaporator. For the condenser, 1,300 mm (or higher in a reasonable range) shell internal diameter is needed and similar tube length is there to the evaporator. With proper adjustment and arrangement for nozzle location and geometry for shell and tube heat exchangers, all fluids can achieve a close value for δ.

As shown in Fig. 6, evaporator shell side heat transfer performance at the bundle point is obtained. The starting bundle point is the shell inlet and the final is near the shell outlet. From Fig. 6, it can be found that there are ten bundle points and as the shell side R134a and its alternatives flow along the shell, the vapor quality increase. The quality of the starting point is ~0.1, which is quite lower than the normal one stage centrifugal chiller system. The adding of the economizer can help to revert the flash gas into the 2nd compressor; thus the quality of working fluids at the inlet of evaporator can be decreased, helping to lift the whole chiller system efficiency. As shown in Fig. 6, all working fluids have similar quality at the starting point and also close value among all the bundle points, with final value to be 1, indicating the superheated compressor suction point. The heat transfer performance shows that with the increasing of the vapor quality, the bundle point shell side heat transfer coefficient gradually increases from bundle point 1 (vapor quality: ~0.1) to point 6 (vapor quality: 0.53-0.55), then it jumps strongly from point 6 to point 8 (vapor quality: ~0.77). After that, the bundle point shell side heat transfer coefficient drops dramatically, from ~3,300 W/m^2·K to ~1,000 W/m^2·K for R134a. All working fluids are following the same trend. Initially, the working fluids have the heat transfer with tube side water, and the baffle help to push the shell-side flow to move forward across the tube bundle, providing the fluid disturbance with zigzag pattern between the tube bundles, which enhances the turbulence intensity, the local mixing, and heat transfer coefficient. The analysis inside the HTRI reveals that the boiling region for bundle points 1-5 is the stratified flow while points 6-8 is the wary-Ann flow. Point 9 is the annular and point 10 is the mist. For the stratified flow, the vapor velocity is low and most dominant fluid state is liquid and the heat

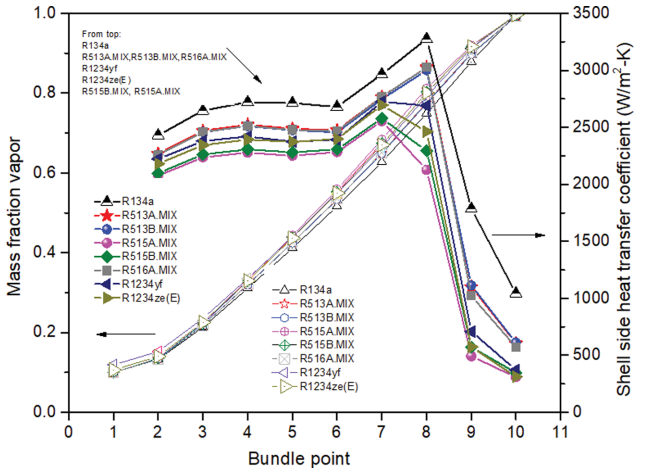

Fig. 6. Evaporator shell side heat transfer performance at the bundle point.

transfer coefficient is only increasing gradually. Then with the help of disturbance inside the shell with baffle and the vapor velocity increases heavily, and the flow region becomes the wary-Ann flow, which can make the heat transfer coefficient lift sharply. Then the velocity increases but most with post dry out, which can seriously decrease the heat transfer performance, as shown from bundle point 8 to point 9 and finally point 10. All working fluids have the same trend for the bundle point heat transfer performance. In addition, R134a displays the highest shell side heat transfer coefficient, followed by R513A, R513B and R516A, then R1234yf and R1234ze(E), and R515B and R515A hold the lowest heat transfer coefficient. The evaporating temperature is 6 °C. For R134a, its saturated liquid density is 1,275 kg/m^3 and others are less than 1,250 kg/m^3; in addition, its saturated liquid thermal conductivity is 89.4 mW/m·K while others mostly are less than 80 mW/m·K. All such properties are favorable for heat transfer for R134a, demonstrating better heat transfer performance than others. Fig. 6 reveals that R513A, R513B and R516A have similar boiling heat transfer characteristics. R515A and R515B display the lowest, indicating more heat transfer areas are needed to achieve the same cooling capacity to the baseline.

Fig. 7 shows the condenser shell side heat transfer performance at the bundle point and the starting bundle point is the shell side inlet. The shell inlet is the 2nd compressor discharge point, with vapor quality to be 1 in the superheated region for the working fluids. Similarly, along the shell side bundle point, all working fluids have the close vapor quality value and finally the working fluids should have the vapor quality to be 0 (not shown in Fig. 7 since it only shows the first 10 bundle points). Regarding the shell side working fluid heat transfer performance, all fluid increases sharply during the first several bundle points, then it decreases gradually. For the first several bundle points, the dropwise condensation for the working fluid from the superheated vapor state to the liquid can sharply increase the heat transfer. Then, gradually, it displays a worsening trend for the heat transfer performance. The HTRI analysis shows that for all working fluids, point 2 is the sensible gas condensate region, point 3 shear, point 4 transition, and all others are the gravity type. A comparison for different fluids shows that R134a is the highest for heat transfer performance, R1234ze(E), R515B and R515A the second, R513A, R513B and R516A the third and final is the R1234yf. Similarly, under the condensing temperature of 36 °C, R134a has the highest liquid density and thermal conductivity than others, demonstrating its better heat transfer performance than others. In addition, similarly, R513A, R513B and R516A have close heat transfer performance for condenser, and the conclusion can also be obtained from aforementioned discussion for the evaporator side. In addition, the subcooled shell side profile is also investigated. The subcooled state means the liquid form for working fluid at different bundle points, as shown in Fig. 8. This is only discussed for the subcooled region. Results show that the liquid film increases first as more vapor condenses, then it decreases gradually. The film heat transfer coefficient is following an increasing trend and R513A and R513B have a better film heat transfer coefficient than other fluids.

Fig. 9 shows the shell side and overall heat transfer performance for both evaporator and condenser. R134a, as the baseline,

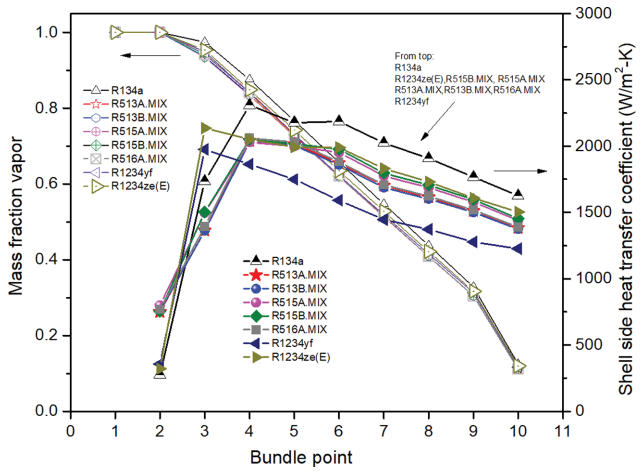

Fig. 7. Condenser shell side heat transfer performance at the bundle point.

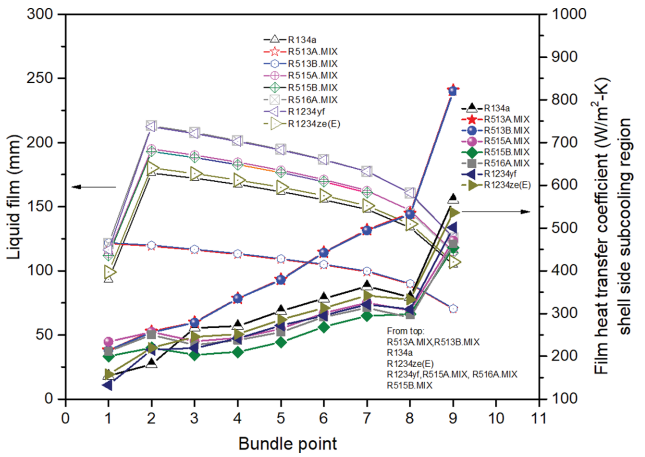

Fig. 8. Condenser shell side subcooling region heat transfer performance.

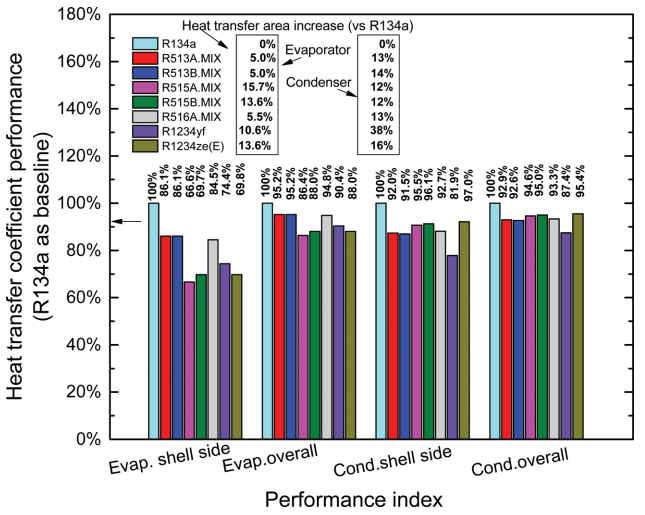

Fig. 9. Evaporator and condenser general heat transfer performance.

shows a value of ~1,550 W/m^2·K for the evaporator shell side and ~1,680 W/m^2·K for the condenser shell side. R134a overall heat transfer coefficient is ~500 W/m^2·K for evaporator and ~830 W/m^2·K for condenser. From Fig. 9, for all performance items, R134a has the best performance. Regarding the evaporator shell side heat transfer coefficient, R513A, R513 B and R516A display ~15% performance drop, while R1234yf 25.6%, R515B 30.3%, R1234ze(E) 30.2% and R515A 33.4%, respectively. Overall performance for the evaporator shows ~5% performance drop for R513A, R513B and R516A, ~10% for R1234yf and ~12% for other fluids. Accordingly, for the evaporator, compared with the baseline for effective heat transfer area, an increase of 5% can be obtained for R513A and R513B, 5.5% for R516A, 10.6% for R1234yf, 15.7% for R515A, 13.6% for R515B and R1234ze(E), respectively. Condenser has a less heat transfer area than evaporator. The most noticeable point is that R1234yf displays ~18% reduction for shell side heat transfer performance and ~13% for the overall performance. The condenser shell side inlet temperature is the compressor discharge temperature and it varies for different refrigerants. Most fluids show a 12-16% condenser heat transfer area increase, while R1234yf can achieve more than 30% area increase. This is mainly caused by its lower discharge temperature for R1234yf (only 41.5 °C) and poor heat transfer performance.

2-2. Centrifugal Chiller

Cycle analyses and compressor sizing have been conducted for R134a and its alternatives under the rating condition (a refrigerant capacity of 1,760 kW with evaporating and condensing temperatures of 6 °C and 36 °C, respectively). The cycle analyses yielded the values for isentropic enthalpy rise and volumetric flow rate needed to determine the speed and compressor impeller diameters. For the two-stage centrifugal chiller, the 1st stage compressor and 2nd compressor cycle analysis have been carried out, as shown in Table 3. The intermediate pressure was chosen to be the optimum pressure from Eq. (1). For all fluids investigated, for the compressor size indicator-impeller diameter, 2nd stage compressor diameter is always less than the 1st one. This is because the 2nd compressor inlet gas density increases, so the 2nd compressor size can be decreased. In fact, the non-equal impeller diameters have performance advantages because non-equal diameters can put more work into higher efficiency stages. For all the mass flow rate ratios for various fluids, the value is quite close. Regarding the pressure ratio, R513A, R513B, R516A and R1234yf have lower value than others.

A screen of the working fluids for the 1st stage compressor size-the impeller diameter shows that R515A, R515B is 19.2% larger for the compressor size from the baseline, R1234ze(E) 15.4%, R1234yf 3.8% and same size for R513A and R513B in comparison with R134a. Similarly, for the 2nd compressor, R515A, R515B and R1234ze(E) can achieve 18.2% larger for compressor size from the baseline, R1234yf 9.1% and all other fluids can obtain same compressor size to R134a. Thus, more modifications are needed for R515A, R515B and R1234ze(E) to obtain the same cooling capacity from the baseline. Impeller tip speed is used to define as the velocity produce at the impeller tip. It is due to the rotation and diameter of the impeller. All fluids have a close value. For the discharge temperature, R134a is highest while R1234yf lowest.

3. Chiller Life Cycle Environmental Performance for Different Working Fluids

This section discusses the life cycle environmental performance with current R134a and its alternatives for two-stage centrifugal chiller system with lifetime of 15 years. For each year in China, take the typical chiller annual operating hours (1,366 h) [36] for the annual electricity consumption calculation. The China electricity emission factor is 0.973 kg CO_2-eq./kW·h [37], which is pretty high since more than 70% of the fuel source type for electricity generation is the high-emission type-coal. For this study, it is also assumed that the same chiller life time energy consumption is consumed in South Korea, for which the electricity emission factor is 0.504 kg CO_2-eq./kW·h [38]. As shown in Fig. 10, the life time

Table 3. Compressor characteristics of R134a and its alternatives

	R134a	R513A	R513B	R515A	R515B	R516A	R1234yf	R1234ze(E)
1st Stage compressor								
Suction superheat [K]	5.0	5.0	5.0	5.0	5.0	5.0	5.0	5.0
Pressure ratio	1.59	1.56	1.56	1.60	1.60	1.55	1.54	1.60
N (Impeller speed) [rpm]	9,465.1	8,804.6	8,768.3	7,463.0	7,532.7	8,972.7	8,078.9	7,731.9
D (Impeller dia.) [m]	0.26	0.26	0.26	0.31	0.31	0.26	0.27	0.30
Head [m]	998.04	883.43	879.28	883.00	892.48	924.70	819.57	919.67
Tip speed [m/s]	127.84	120.28	119.99	120.25	120.89	123.05	115.85	122.72
2nd Stage compressor								
Suction superheat [K]	8.3	6.4	6.3	5.7	5.8	6.4	5.1	6.0
Pressure ratio	1.59	1.56	1.56	1.60	1.60	1.55	1.54	1.60
N (impeller speed) [rpm]	9,619.9	8,847.8	8,807.5	7,527.4	7,601.1	9,020.9	8,067.4	7,812.3
D (Impeller dia.) [m]	0.22	0.22	0.22	0.26	0.26	0.22	0.24	0.26
Head [m]	1,019.87	889.21	884.52	893.17	903.31	931.33	818.01	932.45
Tip speed [m/s]	109.68	103.40	103.16	102.14	102.72	105.97	99.61	104.36
Discharge temperature [°C]	47.92	44.16	44.01	42.41	42.61	44.14	41.55	43.19
Mass flow rate ratio (2nd vs 1st)	1.11	1.13	1.13	1.12	1.12	1.13	1.14	1.12

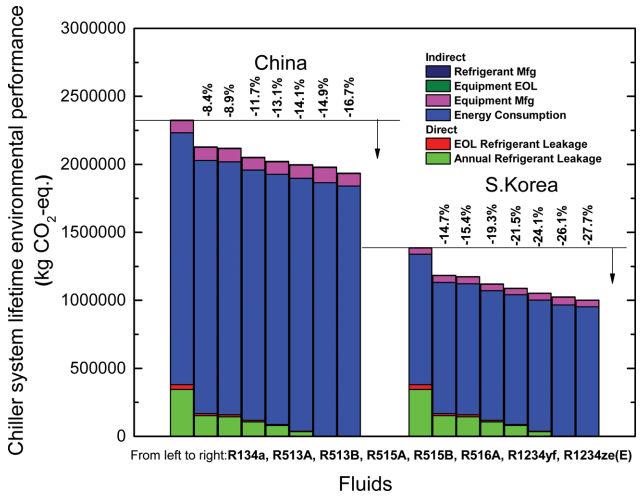

Fig. 10. Chiller lifetime environmental performance under different working fluids.

emission including both the direct and indirect sectors has been compared for China and South Korea. In general, the energy consumption is the largest emission contributor. For China for R134a system, the energy consumption due to annual operation and equipment/refrigerant manufacturing is dominated as 84% for total emission contribution. The direct emissions are 16% from the refrigerant leakage and EOL aspects. Due to the GWP reduction for R134a alternatives, a total emission reduction of 8.4%, 8.9%, 11.7%, 13.1%, 14.1%, 14.9% and 16.7% can be achieved for R513A, R513B, R515A, R515B, R516A, R1234yf and R1234ze, respectively. For R1234yf and R1234ze(E), there is the negligible direct emission due to the extremely low GWP for such two fluids. From such comparison it can be found that the low GWP working fluids help to contribute the environmental protection significantly. From the comparison between China and South Korea it can be concluded that a considerable emission reduction can be achieved for South Korea. Take R134a for example. The same chiller life time emissions in South Korea are a ~40% drop from that in China. A scrutiny of emissions in South Korea reveals that a considerable total emission reduction of 14.7%, 15.4%, 19.3%, 21.5%, 24.1%, 26.1% and 27.7% can be achieved from the baseline R134a for the corresponding low GWP R134a alternative systems. In addition, from this section it is also suggested that the renewable energy or less-emission fuel sources are needed for electricity generation for environmental protection.

CONCLUSIONS

With the growing concern about current HFC refrigerant-R134a for chiller applications, R134a alternatives, such as HFO blends-R513A, R513B, R515A, R515B, R516A and pure HFOs-R1234yf and R1234ze(E), were investigated for two-stage centrifugal chiller application for performance evaluation. The system level thermal performance, component level heat transfer performance/sizing, and life time environmental performance were investigated with a fixed cooling capacity.

With a fixed cooling capacity, all fluids have the equivalent COP. R515A, R515B and R1234ze(E) showing a 25% volume capacity reduction in comparison with baseline due to their low suction density. For the current study, the mass flow rate ratio for the 2nd stage over the 1st stage is approximately 1.1 and the 2nd stage has less volume flow rate due to increased compressor suction inlet gas density. All alternatives have a ~10% or higher mass flow rate.

In general, R134a has a better performance than its alternatives. Regarding the evaporator shell side heat transfer coefficient, R513A, R513B and R516A display ~15% efficient decrease from baseline, R1234yf exhibit 25.6% drop, R515B 30.3%, R1234ze(E) 30.2% and R515A 33.4%, respectively. Regarding the effective evaporator heat transfer area, an increase of 5-5.5% can be obtained for refrigerants of R513A, R513B and R516A, 10.6% increase for R1234yf, 13.6-15.7% enhancement for refrigerant of R515A, R515B and R1234ze(E), respectively. For the condenser side, most fluids show a 12-16% effective heat transfer area increase, while R1234yf over 35%. The comparison for the compressor impeller diameter shows that R513A, R513B and R516A do not require any modifications for compressor size, while R515A, R515B and R1234ze(E) need to replace with a more than 18% larger size compressor. Due to the GWP reduction for R134a alternatives, a total chiller life time emission reduction of 8.4-16.7% was achieved for alternatives from the baseline R134a in China. A more pronounced reduction of 14.7-27.7% can be obtained in South Korea due to the less electricity generation emission factor.

In general, to achieve the same capacity from the baseline R134a, R513A, R513B and R516A have less modification (no compressor change, only heat exchangers needed) and also display the environmental benefits (R513A and R513B do not have better environmental benefits than R516A, but R516A is A2L and necessary vessel safety code protection is needed). Basically, R515A, R515B and R1234ze(E) must experience a large modification for every component (nearly 20% larger size for compressor), indicating more work and cost, but with more environmental benefits. R515A and R515B can serve as an interim non-flammable replacement for R134a in medium-pressure chillers. Finally, with more strict regulations, R1234ze(E) can be the ultimate option in the market with less/negligible modification from R515A and R515B. For R1234yf, in addition to the aforementioned discussions, its high price can also impede its application in chillers, currently not recommended for use.

In addition, in current study, the heat exchanger sizing is mainly performed by the HTRI with shell side refrigerant and tube side water input, and results show that all alternatives display a larger heat transfer area. In the future, more optimization work for heat exchanger considering minimizing the entropy generation [39,40] and downsizing the component size is still needed.

NOMENCLATURE

Abbreviations

ASME : American Society of Mechanical Engineers
CFC : chlorofluorocarbon
COP : coefficient of performance
EOL : End of Life
EPA : Environmental Protection Agency

GHG : greenhouse gas
GWP : global warming potential
HC : hydrocarbon
HCFC : hydrochlorofluorocarbon
IPCC : Intergovernmental Panel on Climate Change
HFC : hydrofluorocarbon
HFO : hydrofluoroolefin
HTFS : Heat Transfer and Fluid Flow Service
HTRI : Heat Transfer Research Inc.
IPLV : Integrated Part-Load Value
ISO : International Standards Organisation
NBP : normal boiling point
TEMA : Tubular Exchangers Manufacturers Association
US : United States

Symbols

A : area [m^2]
D : impeller diameter [m]
D_s : shell diameter [m]
H : head [m]
h : Enthalpy of the state (kJ/kg)
K : annual chiller electricity energy consumption [kW·h]
L : length [m]
LMTD : log-mean temperature difference [°C]
M : refrigerant charge amount [kg]
$\dot{m}_1$: refrigerant mass flow rate at the 1st stage [kg/s]
$\dot{m}_2$: refrigerant mass flow rate at the 2nd stage [kg/s]
N : impeller speed [rpm]
P : pressure of the state [kPa]
P_T : tube pitch [mm]
PR : pressure ratio [-]
Q : heat delivery [kW]
Re_L : Reynold number
U : heat transfer coefficient [$W/m^2 \cdot K$]
V : volume flow rate [m^3/s]
W : power consumption [kW]
ε : void fraction [-]
x : quality [kg/kg]
X_{tt} : correlating parameter

Subscripts

Alter : alternative
1st : first stage
2nd : second stage
1-9 : state as defined in Fig. 2
chill : chilled water
comp : compressor
cond : condenser
cooled : cooled water
dis : discharge
eco : economizer
evap : evaporator
g : gas
HX : heat exchanger
in : inlet
l : liquid
out : outlet
ref : refrigerant
req : required
sat : saturated state
suc : suction state
sub : subcooled state
tp : two phase

REFERENCES

1. J. N. Kang, Y. M. Wei, L. C. Liu, R. Han, B. Y. Yu and J. W. Wang, *Appl. Energy*, **263**, 114602 (2020).
2. G. Li and X. Zheng, *Renew. Sust. Energy Rev.*, **62**, 736 (2016).
3. IPCC, 2013: Summary for Policymakers. In: Stocker, T. F., D. Qin, G.-K. Plattner, et al. Eds. Climate Change 2013: The Physical Science Basis. Contribution of Working Group I to the Fifth Assessment Report of the Intergovernmental Panel on Climate Change. Cambridge, United Kingdom and New York, NY, USA: Cambridge University Press, 2013.
4. Q. Li, L. Zhang, W. Xu, T. Zhou, J. Wang, P. Zhai and P. Jones, *Bull. Am. Meteorol. Soc.*, **98**, 699 (2017).
5. G. Li, *Renew. Sust. Energy Rev.*, **43**, 702 (2015).
6. G. Li, *Sustain. Energy Technol. Assess.*, **11**, 114 (2015).
7. G. Li, *Sustain. Energy Technol. Assess.*, **21**, 33 (2017).
8. IPCC, 2013. Intergovernmental Panel on Climate Change (IPCC), Fifth Assessment Report: Climate Change, Geneva, Switzerland.
9. UN. The Kigali Amendment to the Montreal protocol: another global commitment to stop climate change. https://www.unenvironment.org/news-and-stories/news/kigali-amendment-montreal-protocol-another-global-commitment-stop-climate (accessed March 2020).
10. AGENCY, E.P. Summary Guide to the HFC Phase Down; 2015. Available online: https://www.epa.ie (accessed March 2020).
11. EU Directive 517/2014 Available online: https://www.eea.europa.eu/policy-documents/regulation-eu-no-517-2014 (accessed March 2020).
12. A. U. Atmaca, A. Erek and O. Ekren, *Energy Procedia*, **136**, 394 (2017).
13. E. Navarro, I. O. Mart´ınez-Galvan, J. Nohales and J. Gonzalvez-Macia, *Int. J. Refrigeration*, **36**, 768 (2013).
14. Y. Zhao, Study on the Performance of Automotive Air Conditioning Systems with R1234yf. Ph.D. Thesis, Shanghai Jiao Tong University, Shanghai, China (2012).
15. K. V. Jignesh, *Energy Procedia*, **109**, 153 (2017).
16. T. Aized and A. Hamza, *Arab. J. Sci. Eng.*, **44**, 1697 (2019).
17. Z. Li, H. Jiang, X. Chen and K. Liang, *Energy Build.*, **192**, 93 (2019).
18. C. Aprea, A. Greco, A. Maiorino and C. Masselli, *Int. J. Therm. Sci.*, **127**, 117 (2018).
19. C. Aprea, A. Grecob and A. Maiorino, *Appl. Therm. Eng.*, **141**, 226 (2018).
20. C. Aprea, A. Greco and A. Maiorino, *Int. J. Refrig.*, **82**, 71 (2017).
21. A. Mota Babiloni, J. Navarro Esbri, Á. Barragán Cervera, F. Moles Ribera and B. Peris Pérez, *Int. J. Refrig.*, **51**, 52 (2015).
22. Y. Heredia-Aricapa, J. M. Belman-Flores, A. Mota-Babiloni, J. Serrano-Arellano and J. J. García-Pabón, *Int. J. Refrig.*, **111**, 113 (2020).
23. C. Mateu-Royo, A. Mota-Babiloni, J. Navarro-Esbrí and Á Bar-

ragán-Cervera, *Int. J. Refrig.*, **124**, 197 (2021).
24. P. Johnson and K. Kasai, 2013. System Drop-in Test of R134a Alternative Fluids R-1234ze(E) and D4Y in a 200 RT Air-Cooled Screw Chiller, AHRI low-GWP AREP Report 25, August 2013.
25. K. Ueda, Y. Hasegawa, K. Wajima, M. Nitta, Y. Kamada and A. Yokoyama, *Mitsubishi Heavy Ind. Tech. Rev.*, **49**, 56 (2012).
26. J. J. Brasz, Oil-free Centrifugal Refrigeration Compressors: From HFC134a to HFO1234ze (E). In Proceedings of the 8th International Conference on Compressors and their Systems, London, UK, 9-10 September 2013, pp. 9-10.
27. A. Mota-Babiloni, J. Navarro-Esbrí, A. Barragan, F. Moles and B. Peris, *Appl. Therm. Eng.*, **71**, 259 (2014).
28. A. Sethi and S. Yana Motta, Low GWP Refrigerants for Air Conditioning and Chiller Applications. In Proceedings of the International Refrigeration and Air Conditioning Conference, Purdue University, West Lafayette, IN, USA, 11-14 July 2016; Vol. 2649, pp. 1-8.
29. E. Lemmon, M. Huber and M. McLinden, NIST reference fluid thermodynamic and transport properties REFPROP, version 10.0. The National Institute of Standards and Technology (NIST); 2020.
30. D. Q. Kern, *Process heat transfer*, Tata McGraw-Hill Education, New York (1950).
31. HTRI 2019HTRI. https://www.htri.net/xist. (accessed 19 November 2019).
32. GB/T18430.1-2007: Water Chilling (heat pump) packages using the vapor compression cycle-Part 1: Water chilling (heat pump) packages for industrial & commercial and similar application.
33. E. O. Balje, *Turbomachines, a guide to design, selection and theory*, John Wiley and Sons, New York (1981).
34. K. Schultz and S. Kujak, System Drop-In Tests of R134a Alternative Refrigerants (ARM-42a, N-13a, N-13b, R-1234ze(E), and OpteonTM XP10) in a 230-RT Water-Cooled Water Chiller. Air-Conditioning, Heating, and Refrigeration Institute (AHRI) Low-GWP Alternative Refrigerants Evaluation Program (Low-GWP AREP) report (2013).
35. T. N. Tandon, H. K. Varma and C. P. Gupta, *Int. J. Heat Mass Transf.*, **28**, 191 (1985).
36. M. Zhang, F. Peng and Z. Shi, *Refrig. Air-conditioning*, **10**(6), 11 (in Chinese) (2010).
37. M. Brander, A. Sood, C. Wylie, A. Haughton and J. Lovell, 2011. Electricity-specific emission factors for grid electricity. Ecometrica. <https://ecometrica.com/white-papers/electricity-specific-emission-factors-for-grid-electricity>.
38. Electric Power Statistics Information System. 2017. Facility by Electric Power Source. <http://epsis.kpx.or.kr/epsis/>.
39. Z. Zhang, C. Jiang, Y. Zhang, W. Zhou and B. Bai, *Appl. Therm. Eng.*, **110**, 1476 (2017).
40. Z. Zhang, Y. Zhang, W. Zhou and B. Bai, *Appl. Therm. Eng.*, **94**, 644 (2016).